ACS Catalysis

Research Article

pubs.acs.org/acscatalysis

Highly Active and Stable Co_3O_4/ZSM-5 Catalyst for Propane Oxidation: Effect of the Preparation Method

Zengzan Zhu, Guanzhong Lu,* Zhigang Zhang, Yun Guo, Yanglong Guo, and Yanqin Wang

Key Laboratory for Advanced Materials and Research Institute of Industrial Catalysis, East China University of Science and Technology, Shanghai 200237, China

ABSTRACT: Co_3O_4 supported on ZSM-5 (Co_3O_4/ZSM-5) catalysts were prepared by impregnation (IM), deposition precipitation (DP), and hydrothermal (HT) methods. Their catalytic performances for the total oxidation of propane were tested, and their physicochemical properties were investigated by low-temperature N_2 adsorption, XRD, FT-IR absorption spectroscopy, XPS, H_2-TPR, TEM, and CO chemisorption. The results show that the catalytic activity of Co_3O_4/ZSM-5 for propane oxidation is higher than that of 1.5 wt % Pd/ZSM-5, and the preparation methods remarkably affect the catalytic activity of Co_3O_4/ZSM-5. Among four Co_3O_4/ZSM-5 catalysts prepared by different methods, the catalyst prepared by the HT method possesses the highest catalytic activity for propane oxidation, and their catalytic activities are varied in the order of HT > DP > IM. For the Co_3O_4/ZSM-5 (DP) catalysts, the precipitant has an evident influence on their catalytic activities. For instance, the DP catalyst prepared with ammonium bicarbonate precipitant has a higher catalytic activity than the catalyst prepared with sodium hydroxide precipitant. The excellent catalytic activity of Co_3O_4/ZSM-5 (HT) may be attributed to the better reducibility of Co^{3+}, higher Co^{3+} content, higher surface concentration, and fast migration of the lattice oxygen of Co_3O_4 on this catalyst. Furthermore, the Co_3O_4/ZSM-5 catalyst prepared by the HT method exhibits a high stability after being used at 500 °C for 40 h.

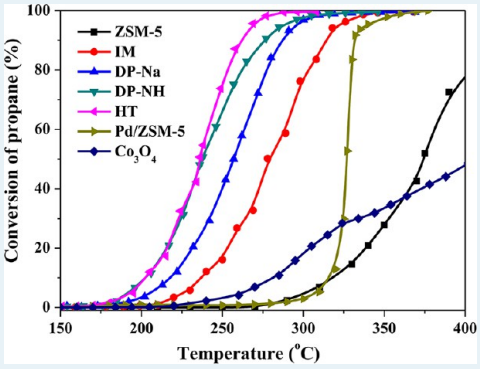

KEYWORDS: *Co_3O_4/ZSM-5, propane oxidation, catalyst preparation, high stability, high activity*

1. INTRODUCTION

In recent years, environmental legislation has imposed increasingly stringent targets for permitted levels of atmospheric emission. Volatile organic compounds (VOCs) as one of the main atmospheric pollutants are evacuated to the atmosphere from a wide variety of gaseous emissions, such as automobile exhaust, petrochemical processes, manufacturing plants, and the treatment of solid and liquid wastes.[1,2] Among the most prevalent VOCs emissions, the release of alkanes (especially light alkanes) to the atmosphere has attracted more and more extensive attention worldwide because the amount of light alkanes released to the atmosphere is increasing as a result of the increasing usage of LPG (primarily composed of propane and butane) and CNG (methane) as a substitute in gasoline and diesel vehicles.[3] In addition, light alkanes are the largest fraction of the hydrocarbon compounds from automobile exhaust, and it is more difficult to remove them from engine exhaust emissions.[4] Moreover, light alkanes released from stationary sources are also increasing with the development of chemical processes and products. Hence, the control of light alkane emissions is very important for a wide range of applications. There are several potential abatement techniques for controlling light alkane emissions, but catalytic oxidation is considered to be one of the most efficient routes.

For the total oxidation of hydrocarbons, noble metal (such as Au, Pt, Pd, Ru) catalysts supported on the oxide with high surface area exhibit excellent activities,[5−7] but the high cost and low availability of noble metals limit their commercial application. To substitute for noble metal catalysts, more attention has been paid to perovskites,[8,9] spinels,[10] hydrotalcites,[11] and single-oxide catalysts (such as copper, manganese, cobalt, nickel, or iron oxide)[12,13] in recent years. In the metal oxide catalysts, cobalt oxide has been demonstrated to be one of the most efficient catalysts for the total oxidation of VOCs,[14,15] and it has the advantages of high activity and low cost compared with noble metal catalysts.

Recently, many efforts have been made to improve the catalytic performance of cobalt oxide by depositing it on a support, such as silica, alumina, titania, magnesia, zeolites, and so on.[16−18] After cobalt oxide is supported, its several properties (such as dispersion, reducibility, electronic structure of smaller cobalt oxide particles, and mechanical and chemical properties) can be obviously improved.[19] The research results show that a high dispersion of cobalt oxide on the support is propitious to increasing its catalytic activity, but it is also easy to interact with the support, resulting in a drop in its reducibility and activity. For example, the strong interaction between cobalt oxide particles and the support for cobalt oxide supported on Al_2O_3 with high

Received: January 28, 2013
Revised: April 14, 2013
Published: April 16, 2013

surface area, such as the formation of the Co−O−Al linkage, is detrimental for propane oxidation.[20] Therefore, a choice of support materials is very important for the cobalt oxide catalyst, and CeO_2, CeO_2−ZrO_2, SBA-15, KIT-5, KIT-6, MCM-41, and MCM-48 have been used as the support for cobalt oxide.[18,21]

Because ZSM-5 zeolite possesses a high thermal stability, high acidity, unique pore structure, and large surface area,[22] it has been widely used as the support in various catalysts, such as Fischer−Tropsch synthesis,[23] N_2O decomposition,[24,25] reduction of NO_x with CH_4,[26] and adsorption (trap/catalyst) of hydrocarbons for reducing cold-start emissions.[27] During the cold-start process in a typical vehicle, 80% of the hydrocarbon (CH_x) emission occurs, in which three-way catalysts used are relatively ineffective for removing the CH_x emission because the catalyst has not reached the light-off temperature. To solve this problem, trapping hydrocarbon by adsorption with a porous catalytic material may be used, and then the hydrocarbon trapped is released and oxidized after this porous catalyst is heated to its light-off temperature by exhaust. To reduce the pollution of released hydrocarbon, this porous catalyst must have high catalytic activity for CH_x catalytic oxidation; that is to say, it can easily reach the light-off temperature of CH_x at the point of desorption temperature. Thus, it is necessary to design and prepare the porous catalyst that can achieve rapid light-off and lower total oxidation temperature for CH_x compounds.

Herein, propane was used as a model gas of light alkanes, and we have an attempt of using ZSM-5 as the support of cobalt oxide to improve its catalytic performance for propane oxidation because ZSM-5 not only has a large adsorption capability for light alkanes (such as propane) but also has a high desorption temperature,[28] which has not been reported as far as we know. Furthermore, there are few papers about the influence of the preparation method on the catalytic activity of Co_3O_4. In this paper, the effects of the preparation methods on the physicochemical properties of cobalt oxide supported on ZSM-5 catalyst were studied in detail, and its catalytic performance was tested for the total oxidation of propane. On the basis of the results obtained, the influences of the preparation methods on the performances of Co_3O_4/ZSM-5 catalysts for propane oxidation have been discussed.

2. EXPERIMENTAL SECTION

2.1. Catalyst Preparation. H-ZSM-5 (Si/Al = 50, BET surface area of 310 m^2/g) was purchased from The Catalyst Plant of Nankai University. The Co_3O_4/ZSM-5 catalysts were prepared by an impregnation (IM), deposition precipitation with sodium hydroxide (DP-Na) or ammonium bicarbonate (DP-NH), and hydrothermal (HT) method, respectively. The theoretical loading of Co was 24.4 wt %. The actual Co loadings in Co_3O_4/ZSM-5 catalysts were measured by inductively coupled plasma (ICP-AES) on a Vanan 710 instrument and are shown in Table 2.

The IM sample was prepared by immersing ZSM-5 into the $Co(NO_3)_2$ (0.5 M) aqueous solution under stirring. The DP samples were prepared as follows: ZSM-5 was added to the $Co(NO_3)_2$ (0.5 M) aqueous solutions under stirring, and NaOH (1 M) or NH_4HCO_3 (2 M) was added slowly to adjust the pH value to 9. After being aged at room temperature for 12 h, the formed solid was filtered and washed with deionized water until pH 7 for the eluate solution. The HT sample was synthesized with the same synthesis solution as for preparing the DP-NH sample, and the hydrothermal preparation condition was at 140 °C for 24 h in a Teflon-sealed autoclave. All catalysts were dried at 120 °C for 12 h and calcined at 500 °C for 3 h under static air in a muffle furnace.

For comparison, bulk cobalt oxide was prepared using the same method as for preparing the DP-Na sample. The catalyst, 1.5 wt % Pd/ZSM-5, was also prepared by impregnating ZSM-5 powder into the 0.5 wt % $Pd(NO_3)_2$ aqueous solution. After being dried at 120 °C overnight, the catalysts were also calcined at 500 °C for 3 h under static air.

2.2. Catalyst Characterization. The surface areas of samples were measured on a Micromeritics ASAP 2400 instrument by N_2 adsorption at −196 °C and calculated by the BET method. The samples were degassed at 180 °C for 12 h before measurement. The *t*-plot method was used to quantitatively determine the micropore volumes of the catalysts. Powder X-ray diffraction (XRD) patterns of catalysts were carried out on a Rigaku D/Max-rC diffractometer with Cu Kα radiation (λ = 1.5418 Å) operated at 40 kV and 40 mA. The scanning electron microscope (SEM) images of samples were obtained on a Hitachi S-3400N microscope operated at 15 kV. The transmission electron microscopy (TEM) images of samples were recorded on a JEOL 2100F electron microscope operated at 200 kV. Fourier transform infrared (FT-IR) absorption spectra were recorded at room temperature on a Nicolet Nexus 670 FT-IR spectrometer with 32 scans at an effective resolution of 4 cm^{-1}. X-ray photoelectron spectroscopy (XPS) spectra were obtained on a VG ESCALAB MK II system equipped with a hemispherical electron energy analyzer. The carbonaceous C1s line (284.6 eV) was used as the reference to calibrate the binding energies (BEs).

Hydrogen temperature-programmed reduction (H_2-TPR) of the sample was carried out in a conventional flow system equipped with a thermal conductivity detector (TCD). The reductant feed consisted of 10 vol % H_2/Ar, and its flow rate was 50 mL/min. The heating rate was 10 °C/min.

The CO chemisorption on the catalyst was tested by means of volumetric pulse techniques. Volumetric chemisorptions were carried out on a Micromeritics AutoChem II 2920 with He as carrier gas of 30 mL/min, and the procedure was the same as that described previously.[29] Before measurement, the samples were reduced under a 10% H_2/N_2 flow (100 mL/min) for 1 h at 400 °C and then flushed with He carrier gas at this temperature for 30 min. After the sample was cooled to room temperature, 10.22 vol % CO pulses (0.5173 mL) were injected into the sample until a saturation of CO adsorption. The Co dispersion was calculated on the basis of the CO−Co chemisorption stoichiometry of 1, and the surface density of 14.6 Co atoms/nm^2 was assumed in the evaluation of Co metal surface area (MSA).[29]

2.3. Catalytic Activity Testing. The catalytic activities of catalysts for propane oxidation were tested in a quartz tube reactor with an inner diameter of 10 mm at atmospheric pressure. The reagent gas consisted of 2000 ppm C_3H_8 + 2% O_2 + the balance made up of N_2 at a flow rate of 100 mL/min. A 200 mg portion of catalyst (40−60 mesh) was used. The reactants and products were analyzed online by gas chromatograph (GC) equipped with a TCD.

2.4. Reaction Kinetics Testing. The kinetics parameters were measured in the fixed-bed reactor for propane oxidation, as mentioned above, which was operated in a differential mode with a C_3H_8 conversion of 5−15%. The catalytic reaction data were obtained after the reaction was stable for 60 min. Both external and internal mass transport limitation can be obviated by varying the catalyst particle size and W/F (the ratio of catalyst weight to total flow rate). For instance, both external and internal mass

dx.doi.org/10.1021/cs400068v | ACS Catal. 2013, 3, 1154−1164

Table 1. BET Surface Area, Pore Volumes and Crystallite Sizes of Co_3O_4/ZSM-5 Catalysts

catalyst	S_{BET} (m^2/g)[a]	micropore S_{BET} (m^2/g)	total pore vol (mL/g)	micropore vol (mL/g)	crystallite size of Co_3O_4 (nm)[b]
ZSM-5	310	288	0.181	0.142	
IM	127	113	0.082	0.056	31.2
DP-Na	182	166	0.125	0.083	16.4
DP-NH	225	195	0.192	0.096	16.9
HT	231	198	0.224	0.10	35.4
Co_3O_4	28				19.4
Pd/ZSM-5	290	262		0.123	

[a]Total surface area was determined by the BET method. [b]Calculated through the XRD patterns by Scherrer equation.

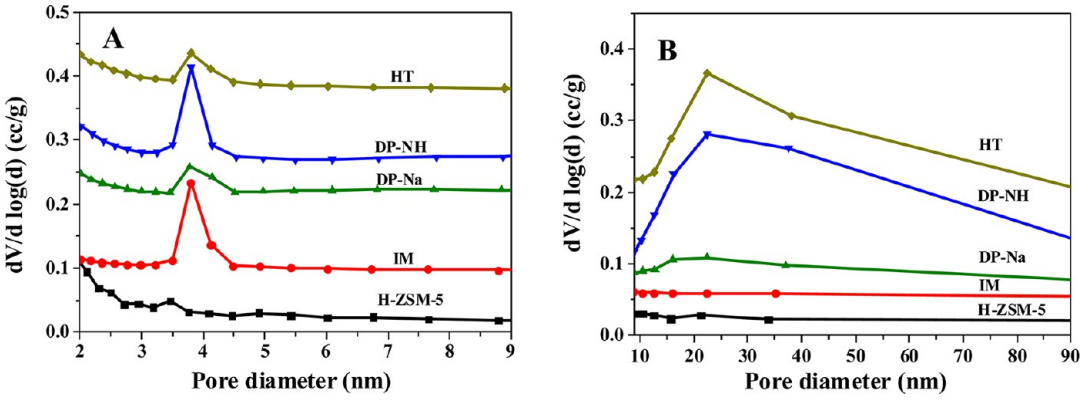

Figure 1. Pore-size distribution curves of Co_3O_4/ZSM-5 catalysts prepared by different methods.

transfer resistance were eliminated when a feed gas flow rate reached 150 mL/min and the catalyst particle size was minished to 60−80 mesh. The conversion of propane is calculated as eq 1,

$$X_{C_3H_8} = \frac{[C_3H_8]_{in}\ \text{vol}\ \% - [C_3H_8]_{out}\ \text{vol}\ \%}{[C_3H_8]_{in}\ \text{vol}\ \%} \quad (1)$$

where $[C_3H_8]_{in}$ and $[C_3H_8]_{out}$ are the C_3H_8 concentrations in the inlet and outlet gas (vol %), respectively. The reaction rate, $r_{C_3H_8}$ (mol/($g_{Co_3O_4}$·s)), is calculated with $X_{C_3H_8}$ as eq 2,

$$r_{C_3H_8} = \frac{N_{C_3H_8} \cdot X_{C_3H_8}}{W_{cat}\ w\%_{Co_3O_4}} \quad (2)$$

where $N_{C_3H_8}$ is the C_3H_8 gas flow rate (mol/s), W_{cat} is the catalyst weight (g), $w\%_{Co_3O_4}$ is the content of Co_3O_4 in the Co_3O_4/ZSM-5 catalyst.

When the conversion of propane is <15%, a dependence of the reaction rate ($r_{C_3H_8}$) on the products of CO_2 and H_2O may be ignored; hence, the empirical kinetic expression of the reaction rate equation of C_3H_8 oxidation can be described as eq 3.

$$r_{C_3H_8} = A \exp\left(-\frac{E_a}{RT}\right) P_{C_3H_8}^{\alpha} P_{O_2}^{\beta} \quad (3)$$

Taking the logarithm of eq 3, eq 4 can be obtained.

$$\ln r = \ln A + \alpha \ln P_{C_3H_8} + \beta \ln P_{O_2} - E_a/(RT) \quad (4)$$

The components of the reactant feed gas are hardly changed during the kinetics data testing, and the conversion of propane is <15%. Therefore, ln A, $\alpha \ln P_{C_3H_8}$, and $\beta \ln P_{O_2}$ can be supposed to be approximately constant, and eq 4 can be simplified to $\ln r = -E_a/(RT) + C$. The activation energy (E_a) can be obtained from the slope of the resulting linear plot of ln r versus $1/T$.

3. RESULTS AND DISCUSSION

3.1. Structural and Textural Properties of Catalysts.

The structural and textural properties of Co_3O_4/ZSM-5 catalysts prepared by different methods are shown in Table 1. It can be observed that all Co_3O_4/ZSM-5 catalysts have a lower BET surface area than the ZSM-5 support, which is attributed to a clogging or covering of the pores of ZSM-5 support by loaded Co_3O_4. The BET surface area of the Co_3O_4/ZSM-5 catalyst obviously depends on the preparation method. The IM catalyst has the lowest surface area (127 m^2/g) among these Co_3O_4/ZSM-5 samples because Co species can easily migrate and accumulate during the thermal treatment for the wetness impregnation sample. The surface area of the catalyst prepared by the DP method is related to the used precipitant, and the BET surface area of the DP-NH catalyst prepared with NH_4HCO_3 precipitant is larger than that of the DP-Na catalyst prepared with NaOH precipitant because sodium was proven to be a sintering agent, even at a very low concentration.[30] A similar situation was also observed in the red mud hydrogenation catalyst (Fe, Ti, Al, etc. mixed oxide).[31,32] The BET surface area (231 m^2/g) of the HT catalyst is slightly higher than that of the DP-NH sample, which may be the polymerization/condensation of cobalt species on the support surface at 140 °C hydrothermal temperature, resulting in less Co_3O_4 species entering into the pores. It is also observed that the change sequence of total and micropore volumes is the same as that of the surface areas of Co_3O_4/ZSM-5 catalysts.

The pore-size distribution curves of Co_3O_4/ZSM-5 samples are determined by the BJH method on the basis of the desorption branch and are shown in Figure 1. It can be seen that the preparation method obviously affects the pore-size distributions of the Co_3O_4/ZSM-5 samples. As shown in Figure 1A, there are mainly pores of <2.5 nm and fewer pores of ~3.5 nm in the ZSM-5 support, and there are more pores of 3.5−4.5 nm in the Co_3O_4/ZSM-5 samples, which may be attributed to the internal pores of

dx.doi.org/10.1021/cs400068v | ACS Catal. 2013, 3, 1154−1164

cobalt oxide particles. For the Co_3O_4/ZSM-5 catalysts prepared by the DP and HT methods, a new broader distribution peak of pore size at 10−80 nm can be observed in Figure 1B and may be attributed to the accumulated hole between particles by nano-Co_3O_4 crystallite bridges.

Figure 2 shows powder XRD patterns of Co_3O_4/ZSM-5 catalysts. The diffraction peaks of the spinel phase Co_3O_4 are

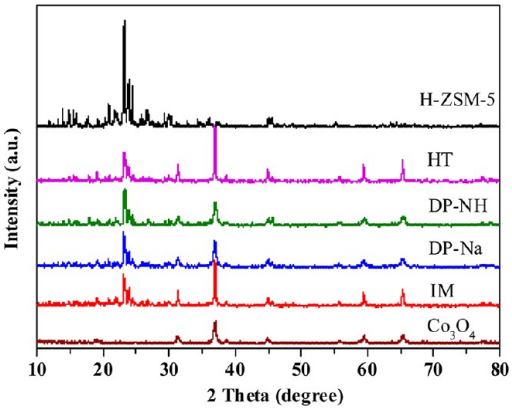

Figure 2. XRD patterns of Co_3O_4/ZSM-5 catalysts prepared by different methods.

observed at 2θ = 19.0°, 31.3°, 37.0°, 59.5°, and 65.4°, corresponding to the (111), (220), (311), (511), and (440) crystal faces. No characteristic peaks of the CoO phase at 2θ = 34.1°, 39.5°, 57.2°, and 68.4° are observed. The crystallite sizes of Co_3O_4 in Co_3O_4/ZSM-5 catalysts are calculated from the Co_3O_4 (311) diffraction peak by the Scherrer equation and shown in Table 1. It can be seen that the crystallite size of the DP catalysts is 16−17 nm, and only half crystallite sizes of IM (31.2 nm) and HT (35.4 nm) catalysts. For the IM catalyst, because of a relatively weak interaction between the metal precursor and the ZSM-5 support in the process of impregnating ZSM-5 in the Co^{2+} aqueous solution, cobalt species can be redistributed during drying and calcination, resulting in an aggregation of cobalt oxide on the ZSM-5 support. The pH of the impregnation solution can also affect the sizes of cobalt oxide particles on the support.[19] Although the pH of the synthesis solution for the HT catalyst is the same as the DP catalyst, Co_3O_4 crystallites can grow on the support under hydrothermal conditions. Therefore, the HT catalyst has a larger crystallite size than the catalysts prepared by the DP method.

The SEM images of Co_3O_4/ZSM-5 catalysts are shown in Figure 3, and the difference in morphology (a random particle) between catalysts can be observed unobviously; however, the small particles attached to large particles are unalike for catalysts prepared by different methods. The small particles of the IM catalyst are spherical, and their sizes are ∼300 nm and larger than that of DP-Na, DP-NH, and HT catalysts, which are nanoparticles. In the DP and HT catalysts, loose cobalt oxide nanoparticles are obviously observed, especially for the DP-NH and HT catalysts, resulting in much higher surface areas of DP-NH and HT catalysts than other Co_3O_4/ZSM-5 catalysts.

The TEM images in Figure 4 show that the particle sizes of Co_3O_4/ZSM-5 are affected by the preparation method. The IM catalyst presents the densely spherical particles of ∼350 nm (Figure 4a) and may be an aggregate of many small crystallites of cobalt oxide. For the DP-Na catalyst, many cobalt oxide nanoparticles of ∼10 nm are attached on the catalyst, and

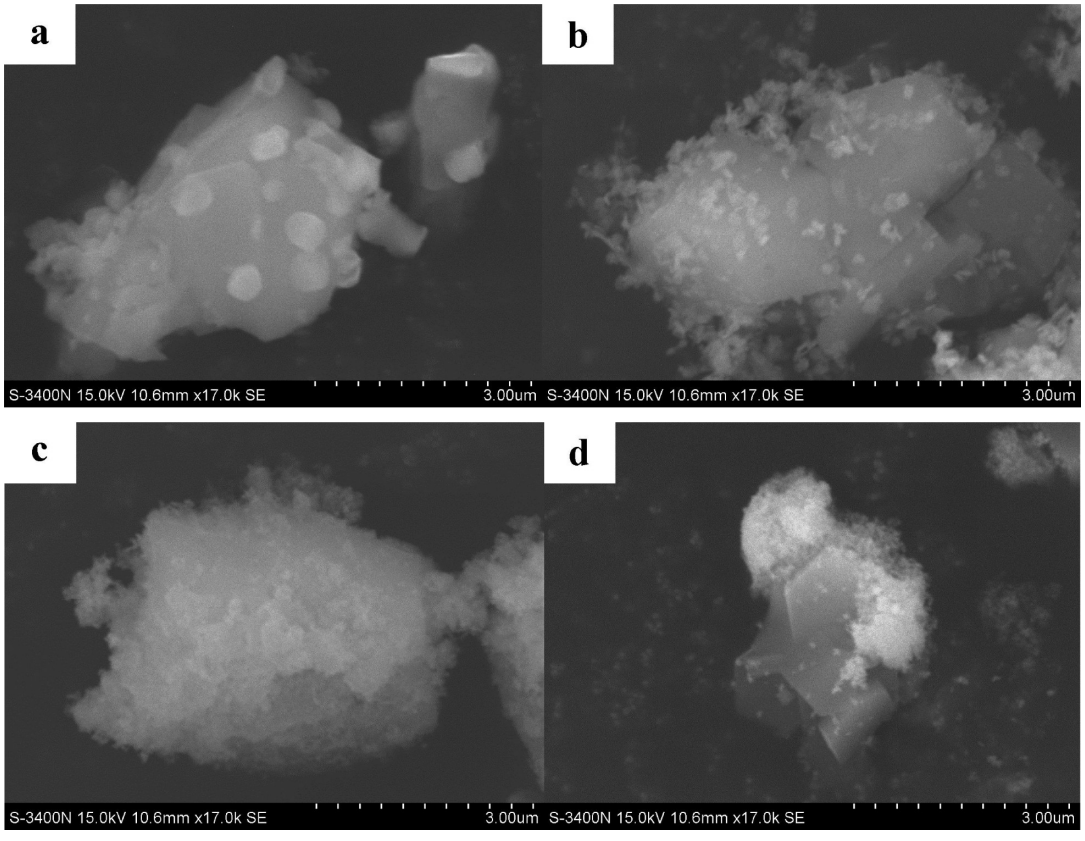

Figure 3. SEM images of (a) IM, (b) DP-Na, (c) DP-NH, and (d) HT catalysts.

dx.doi.org/10.1021/cs400068v | ACS Catal. 2013, 3, 1154−1164

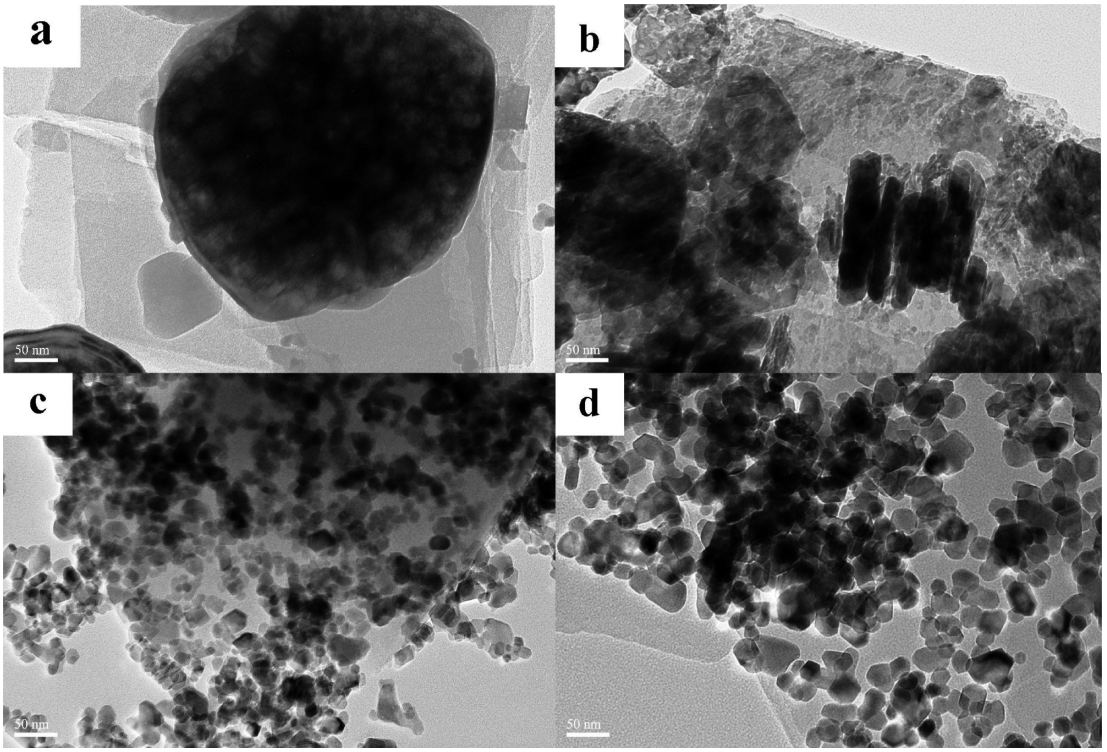

Figure 4. TEM images of (a) IM, (b) DP-Na, (c) DP-NH, and (d) HT catalysts.

some large rodlike (100−150 nm) and polygon particles are also observed (Figure 4b). The DP-NH and HT catalysts have similar particle distributions, and the particle size of the DP-NH catalyst is smaller than that of the HT catalyst attached to more uniform particles of ∼30 nm.

3.2. Temperature-Programmed Reduction and CO Chemisorption. The reduction behavior of Co_3O_4/ZSM-5 catalysts was investigated, and the results are shown in Figure 5.

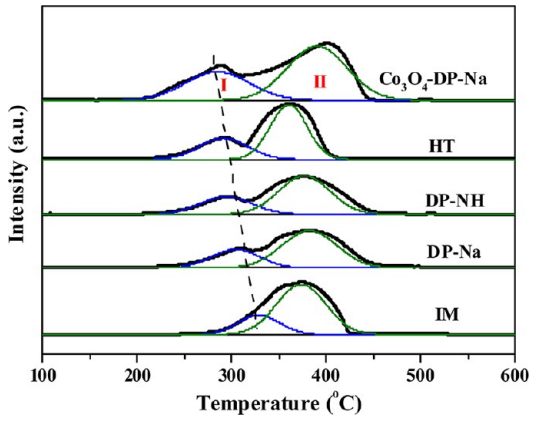

Figure 5. TPR profiles of Co_3O_4/ZSM-5 catalysts prepared by different methods.

With respect to the reduction process of Co_3O_4, there are various controversial viewpoints. Arnoldy et al.[33] considered a single-step reduction of Co_3O_4, but many researchers[34−36] reported that the reduction of Co_3O_4 was a two-step process involving the intermediate reduction of CoO. There are two distinct reduction peaks at <450 °C in the TPR profiles of Co_3O_4/ZSM-5 catalysts in Figure 5, and the intensity of peak I is obviously lower than that of peak II, which is consistent with the reduction behavior of fine Co_3O_4 particles;[37,38] however, it was also reported that the peak at low temperature is associated with the reduction of Co^{3+} to Co^{2+} with concomitant structural changes of the sample to CoO, and the peak at high temperature is the subsequent reduction of CoO to metallic cobalt.[39,40] Herein, we think, peak I is attributed to the reduction of Co^{3+} to Co^{2+}, and peak II is ascribed to the reduction of CoO to metallic cobalt.

A quantitative evaluation of hydrogen consumption shows that Co_3O_4 is reduced almost completely (Table 2), and the ratios of Co^{3+}/Co^{2+} calculated by $area_{peak\ I}/area_{peak\ II}$ and the relative contents of Co^{3+} ($Co^{3+}/(Co^{3+} + Co^{2+})$) are also shown in Table 2. The results show that the preparation method obviously influences the relative content of Co^{3+} and the ratio of Co^{3+}/Co^{2+} in the Co_3O_4/ZSM-5 catalyst. The HT catalyst shows the highest relative content of Co^{3+} (33.9%) and ratio of Co^{3+}/Co^{2+} (51.2%). The relative content of Co^{3+} and the ratio of Co^{3+}/Co^{2+} for Co_3O_4/ZSM-5 catalysts are varied in the order of HT > DP-NH > DP-Na > IM.

For the reduction of Co^{3+} (peak I) in the TPR profiles (Figure 5), the HT catalyst has the lowest reduction temperature (∼290 °C) among all Co_3O_4/ZSM-5 catalysts, and the reduction temperature of the IM catalyst is the highest (∼326 °C); the reduction temperatures of other catalysts are changed in the order of HT < DP-NH < DP-Na < IM (Table 2). For the reduction of CoO to metallic cobalt (peak II), the reduction temperature of Co_3O_4/ZSM-5 catalyst is increased in the order of HT < IM < DP-NH < DP-Na, and the Co_3O_4 particle size on ZSM-5 is similarly decreased. It was reported that the particle size effect is typical for the second reduction peak of CoO to metallic cobalt, and larger particles are reduced more easily in comparison with smaller particles.[27,40]

The Co dispersions on Co_3O_4/ZSM-5 catalysts calculated by CO chemisorption are summarized in Table 3. All Co_3O_4/ZSM-5 catalysts exhibit a very low Co dispersion of 0.41−0.63%, resulting in a low surface area of Co metal (only 0.82−1.06 m^2/

dx.doi.org/10.1021/cs400068v | ACS Catal. 2013, 3, 1154−1164

Table 2. Cobalt Contents, Top Temperatures of Reduction Peaks, H_2 Uptakes, Relative Co^{3+} Contents and Co^{3+}/Co^{2+} of Co_3O_4/ZSM-5 Catalysts

catalyst	Co loading (wt %)[a]	top temp peak I/peak II (°C)	H_2 uptake (μmol/g)	reduced Co_3O_4 (wt %)[b]	Co^{3+}/Co^{2+} (%)	$Co^{3+}/(Co^{3+}+Co^{2+})$ (%)[c]
ZSM-5			156			
IM	24.0	326/372	5316	97.9	32.7	24.6
DP-Na	24.4	306/378	5381	97.5	43.6	30.4
DP-NH	23.7	300/375	5107	95.3	46.5	31.7
HT	24.3	290/361	5386	98.0	51.2	33.9
1.5% Pd/ZSM-5	1.36					

[a]Evaluated by ICP-AES. [b]The amount of Co_3O_4 reduced has been calculated on the basis of the total H_2 consumption, assuming that complete reduction of $Co_3O_4 \rightarrow Co$ occurs. [c]The relative content of Co^{3+} was calculated by $[\text{area}_{\text{peak I}}/(\text{area}_{\text{peak I}} + \text{area}_{\text{peak II}}) \times 100\%]$.

Table 3. CO Chemical Adsorption Amounts (CAA), Cobalt Dispersions and Cobalt Surface Areas of Co_3O_4/ZSM-5 Catalysts

catalyst	CO CAA (μmol/g_{cat})	D_{Co} (%)[a]	Co surface area (m^2/g_{cat})[b]
IM	25.6	0.63	1.06
DP-Na	17.1	0.41	0.70
DP-NH	23.7	0.59	0.98
HT	19.7	0.48	0.82
1.5Pd/ZSM-5[c]	33.6	2.61	6.1

[a]The cobalt dispersion (D_{Co}) was calculated using $[(\text{mol}_{\text{COadsorbed}}/\text{mol}_{Co}) \times 100\%]$. [b]The Co metal surface area was calculated by assuming a Co surface density of 14.6 Co atoms/nm^2. [c]The Pd metal surface area was calculated by assuming a Pd molar surface area of 47780 m^2/mol.[41]

g_{cat}), which may be attributed to the high cobalt loading of ~24%. Among the Co_3O_4/ZSM-5 catalysts prepared by different methods, the IM catalyst shows the highest Co dispersion because some Co^{2+} ions may be exchanged for H^+ ions in the ZSM-5 support during the process of immersing ZSM-5 into the $Co(NO_3)_2$ (0.5 M) aqueous solution at 80 °C under stirring for 2 h. Therefore, a small quantity of Co^{2+} ions enter into the inner pores of ZSM-5, which does not affect the crystallite sizes of Co_3O_4 located in outer surface of ZSM-5 support, but can increase the dispersion of Co.

3.3. FT-IR Absorption Spectroscopy. The FT-IR absorption spectra of Co_3O_4/ZSM-5 catalysts are shown in Figure 6. Two absorption bands at 667 and 575 cm^{-1} are observed in the IR spectrum of cobalt oxide, which is in accordance with the stretching vibration of metal-oxide bond in the Co_3O_4 spinel lattice.[42] For the Co_3O_4/ZSM-5 catalysts, the band at 664–668 cm^{-1} can be assigned to the stretching vibration mode of M–O (M is tetrahedrally coordinated Co^{2+}), and the band at 565–577 cm^{-1} can be attributed to the stretching vibration of M–O (M is octahedrally coordinated Co^{3+}).[43,44] As shown in Figure 6, the stretching vibration band of octahedrally coordinated Co^{3+} at 575 cm^{-1} is changed in the order of IM (575 cm^{-1}) > DP-Na > DP-NH > HT (565 cm^{-1}), which indicates a decrease in the strength of the Co–O bond in Co_3O_4; that is to say, the reduction of Co^{3+} becomes easy. The results above are consistent with the TPR results (Figure 5); that is, the Co^{3+} reduction temperature shifts to lower temperature in the same order as the wavenumber shift in their IR spectra for the four Co_3O_4/ZSM-5 catalysts.

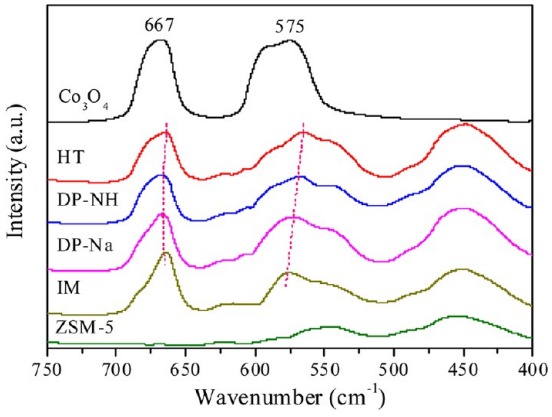

Figure 6. FT-IR spectra of Co_3O_4/ZSM-5 catalysts prepared by different methods.

For the tetrahedrally coordinated Co^{2+} species, the IM catalyst has almost the same stretching vibration absorption as the HT catalyst; however, the stretching vibration band for DP catalysts shifts slightly toward a higher wavenumber when compared with that of the IM and HT catalysts, which indicates that the strength of the Co–O bond for the DP catalysts is stronger and more difficult to be reduced than the IM and HT catalysts. Therefore, the reduction peak of Co^{2+} for DP catalysts shifts to a higher temperature in the TPR profiles (Figure 5). The vibration band at 450 cm^{-1} for Co_3O_4/ZSM-5 is also presented in the IR spectrum of ZSM-5 support, so it can be attributed to the bending vibration of T-O (T is Si or Al).[45]

3.4. X-ray Photoelectron Spectroscopy (XPS). The Co_3O_4/ZSM-5 catalysts were investigated by XPS to examine the influence of the preparation method on their surface chemical states. The XPS spectra of Co 2p and O 1s are shown in Figure 7, and the XPS data are summarized in Table 4. In the Co 2p XPS spectra (Figure 7A), the peaks located at 795.5–796.1 and 780.3–780.9 eV may be ascribed to Co $2p_{1/2}$ and Co $2p_{3/2}$ spin–orbital peaks, respectively. It is well-known that the spin–orbit splitting value for Co^{3+} compounds is 15.0 eV,[11] and for the mixed-valence Co_3O_4, its spin–orbit splitting value is 15.1–15.3 eV.[19,43,46] Here, the spin–orbit splitting value of Co 2p for Co_3O_4/ZSM-5 catalysts is 15.2 ± 0.1 eV (Table 4), which is close to that of mixed-valence Co_3O_4, so that the cobalt species on Co_3O_4/ZSM-5 should be Co_3O_4.

The results in Table 4 show that the preparation method has an obvious influence on the surface compositions of Co_3O_4/ZSM-5 catalysts. For instance, the IM catalyst has the lowest surface cobalt content (3.57%) among all Co_3O_4/ZSM-5 catalysts; for DP-Na and DP-NH catalysts prepared by the coprecipitation method, cobalt enrichment on the surface can be observed, which is similar to the results reported by Luo et al.[46] The surface cobalt content on the HT catalyst is 8.94%, which may be ascribed to the polymerization/condensation of cobalt

dx.doi.org/10.1021/cs400068v | ACS Catal. 2013, 3, 1154–1164

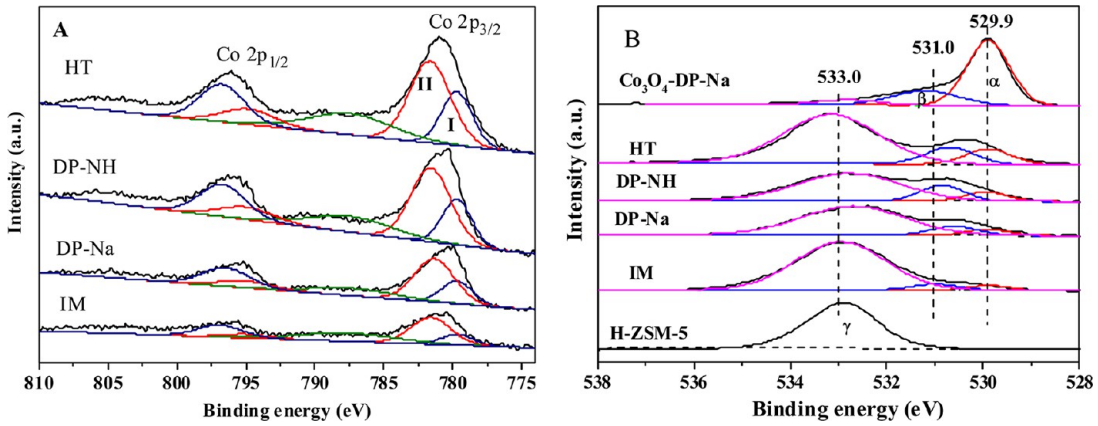

Figure 7. XPS spectra of Co 2p (A) and O 1s (B) of Co_3O_4/ZSM-5 catalysts.

Table 4. XPS Data of Co_3O_4/ZSM-5 Catalysts Prepared by Different Methods

		surface content (%)[b]				
sample	binding energy (eV)[a] Δ (Co $2p_{3/2}$–Co $2p_{1/2}$)	Co 2p	Co^{3+}/Co^{2+}	$Co^{3+}/(Co^{3+}+Co^{2+})$	O_α	O_β
IM	15.1 (795.5–780.4)	3.57	31.2	23.8	2.6	3.7
DP-Na	15.3 (795.6–780.3)	4.83	40.3	28.7	4.6	7.5
DP-NH	15.3 (795.8–780.6)	7.67	45.2	31.2	6.2	11.0
HT	15.2 (796.1–780.9)	8.94	49.1	32.9	7.3	8.5

[a]The difference (Δ) of binding energy between Co $2p_{3/2}$ and Co $2p_{1/2}$. [b]The ratio of Co^{3+}/Co^{2+} was calculated from "peak I area/peak II area" in Figure 7; O_α is the surface lattice oxygen concentration; O_β is the surface adsorbed oxygen concentration.

species on the surface in the hydrothermal preparation process at 140 °C. Furthermore, the Co 2p spectra can be fitted to the Co^{2+} and Co^{3+} components on the basis of the restriction that Co $2p_{3/2}$ binding energies of Co^{2+} and Co^{3+} components are 781.5 ± 0.2 and 779.6 ± 0.1 eV, respectively. The spin–orbit doublet splitting is set to 15.2 ± 0.1 eV with a fixed ratio of 2/1 for the $2p_{3/2}$-to-$2p_{1/2}$ peak area. The surface content ratios of Co^{3+}/Co^{2+} and the relative surface contents of Co^{3+} ($Co^{3+}/(Co^{3+} + Co^{2+})$) are also listed in Table 4. It is interesting that the Co^{3+}/Co^{2+} and $Co^{3+}/(Co^{3+} + Co^{2+})$ values for four Co_3O_4/ZSM-5 catalysts in Table 4 are almost the same as the results from TPR (Table 2), and their difference is very small (Figure 8). Therefore, it can be concluded that the preparation method obviously influences the relative surface content of Co^{3+} and the surface content ratio of Co^{3+}/Co^{2+} on the Co_3O_4/ZSM-5 catalyst, and their relative surface content of Co^{3+} and the surface content ratio of Co^{3+}/Co^{2+} are varied in the order of HT > DP-NH > DP-Na > IM.

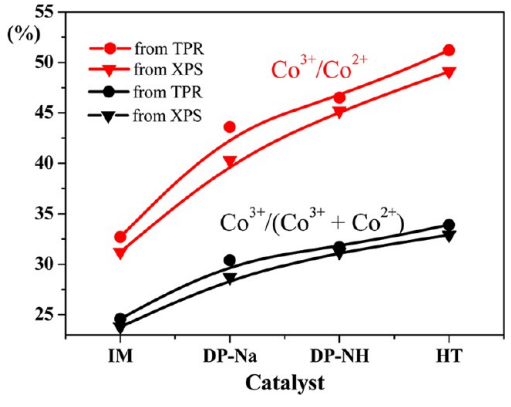

Figure 8. The difference for $Co^{3+}/(Co^{3+}+Co^{2+})$ and Co^{3+}/Co^{2+} between data obtained by TPR and XPS.

The O 1s XPS spectra of Co_3O_4/ZSM-5 catalysts are shown in Figure 7B. In the O 1s XPS spectrum of H-ZSM-5, only one peak (γ) at ~532.8 eV can be observed, which may be assigned to the lattice oxygen (O_γ) of the ZSM-5 support.[47,48] For the Co_3O_4 sample, there are two peaks (α, β) in its O 1s XPS spectrum. The α peak at ~529.9 eV is attributed to the surface lattice O^{2-} (O_α) of Co_3O_4, and the β peak at ~531 eV is attributed to adsorbed oxygen species (O_β).[49] In the O 1s XPS spectra of the Co_3O_4/ZSM-5 catalysts, the oxygen species of the γ peak at ~532.8 eV is assigned to the oxygen of ZSM-5 support, and the contents of O_α and O_β on the Co_3O_4/ZSM-5 samples are varied with the different preparation methods; their data are shown in Table 4. It is obvious that the HT sample has a higher surface O_α content (7.3%) than other samples, and the surface content of O_α on the IM catalyst is lowest. Although the DP catalysts have a moderate O_α content when compared with the HT and IM catalysts, different precipitants have an obvious influence on the O_α content of the DP catalysts. For instance, the DP-NH catalyst prepared with ammonium bicarbonate exhibits a higher O_α content than those over the DP-Na catalyst prepared with sodium hydroxide. However, for the surface adsorbed oxygen species (O_β), the DP-NH catalyst shows the highest O_β content (11.0%), and the IM catalyst still has the lowest O_β content (3.7%) among the Co_3O_4/ZSM-5 catalysts.

3.5. Performances of Co_3O_4/ZSM-5 Catalysts for Propane Oxidation. The catalytic performances of Co_3O_4, Co_3O_4/ZSM-5, and Pd/ZSM-5 catalysts for propane oxidation are shown in Figure 9, and T_{50} and T_{90} (the reaction temperatures of 50 and 90% propane conversion) are listed in Table 5. The results show that the Co_3O_4/ZSM-5 catalysts demonstrate a much higher catalytic activity than Pd/ZSM-5, pure ZSM-5, and Co_3O_4 samples for propane oxidation. For instance, T_{50} and T_{90} over the Pd/ZSM-5 catalyst are 326 and 332 °C, and T_{50} and T_{90} over the HT catalyst are 235 and 260 °C, respectively. For Co_3O_4/ZSM-5 catalysts, the preparation

dx.doi.org/10.1021/cs400068v | ACS Catal. 2013, 3, 1154–1164

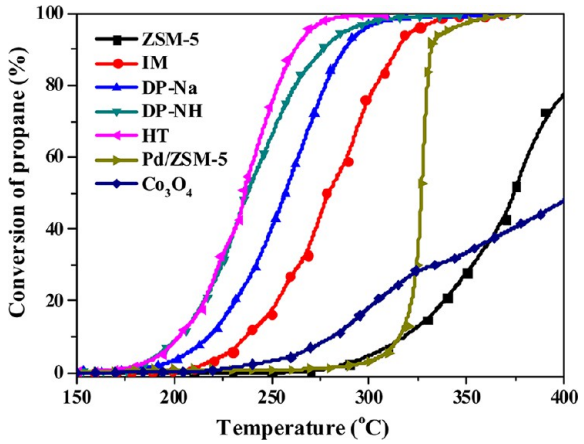

Figure 9. The catalytic performances of ZSM-5, Co_3O_4, Co_3O_4/ZSM-5, and Pd/ZSM-5 catalysts for propane oxidation.

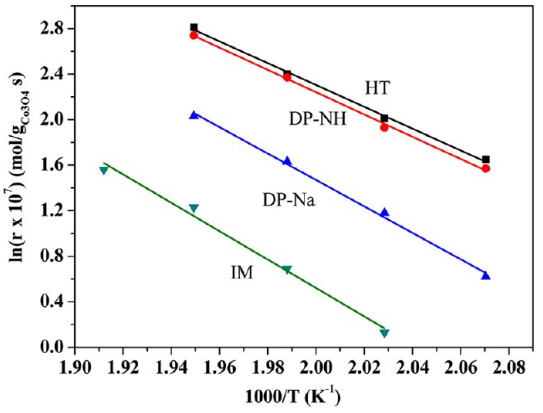

Figure 10. Arrhenius plots (ln ($r \times 10^7$) vs 1000/T) over the Co_3O_4/ZSM-5 catalysts for propane oxidation.

method seriously influences its catalytic activity for propane oxidation. For instance, the catalyst prepared by the HT method exhibits the lowest T_{50} (235 °C) and T_{90} (260 °C), which are much lower than the supported Co_3O_4 catalysts reported.[15,50] For the DP catalysts prepared by a deposition precipitation method, the precipitant has an evident influence on its catalytic activity: the activity of DP-NH catalyst is close to that of the HT catalyst and much higher than that of the DP-Na catalyst. Although T_{50} (277 °C) and T_{90} (314 °C) over the IM catalyst are much higher than those over the DP catalysts, its T_{50} and T_{90} are nearly 50 and 20 °C lower than those over the Pd/ZSM-5 catalyst. For the deep oxidation of propane over the Co_3O_4/ZSM-5 catalysts, the catalytic activity order is HT > DP-NH > DP-Na > IM.

The reaction rates of Co_3O_4 and Co_3O_4/ZSM-5 catalysts at 230 °C and the rate of Pd/ZSM-5 at 280 °C were measured, and the results are shown in Table 5. Figure 10 shows Arrhenius plots of ln r versus $1/T$ for the Co_3O_4/ZSM-5 catalysts, and the activation energies (E_a) obtained from the slopes of the resulting linear plots of ln r versus $1/T$ are listed in Table 5. The results show that the apparent E_a for propane oxidation over the Co_3O_4/ZSM-5 catalysts is 79.7−104 kJ/mol, and the Co_3O_4/ZSM-5 catalysts exhibit much higher reaction rates ($r = 3.67 \times 10^{-7}$ mol/(g_{cat}·s)) at 230 °C than the Pd/ZSM-5 catalyst ($r = 0.12 \times 10^{-7}$ mol/(g_{cat}·s)) at 280 °C. Among the Co_3O_4/ZSM-5 catalysts, the HT catalyst shows a slightly higher catalytic activity for propane oxidation than the DP-NH catalyst, and its reaction rate reaches 11.1×10^{-7} mol/($g_{Co_3O_4}$·s) at 230 °C and obviously higher than the DP-Na (5.09×10^{-7} mol/($g_{Co_3O_4}$·s)) and IM catalyst (1.99×10^{-7} mol/($g_{Co_3O_4}$·s)). Their reaction rates of catalyzing propane oxidation are ranked as follows: $r_{HT} > r_{DP\text{-}NH} > r_{DP\text{-}Na} > r_{IM}$, and the same order is also observed in Table 5 as normalized to a specific rate per mass unit or surface area unit. The results above indicate that the Co_3O_4/ZSM-5 catalyst prepared hydrothermally exhibits a much higher catalytic activity for propane oxidation than other Co_3O_4/ZSM-5 catalysts.

Furthermore, the reaction rates over the HT (11.1×10^{-7} mol/($g_{Co_3O_4}$·s)) and DP-NH (10.7×10^{-7} mol/($g_{Co_3O_4}$·s)) catalysts at 230 °C are much higher than those over Co/TiO_2 (2.24×10^{-7} mol/ ($g_{Co_3O_4}$s)) and Co/Al_2O_3 (0.40×10^{-7} mol/ ($g_{Co_3O_4}$·s)) at 300 °C[15] in the reactant gas of 0.5% propane/air with 50 mL/min. The superior catalytic activity of HT and DP-NH catalysts, which possess a lower E_a for propane oxidation, may be correlated with the higher surface cobalt content (Table 4) and the easy reduction of surface Co^{3+} ions (Figure 5) or higher surface lattice oxygen concentration of Co_3O_4 (O_α in Figure 7), resulting in facile adsorption and activation of the reactants.

The results in Table 5 show also that TOFs of Co_3O_4/ZSM-5 catalysts at 230 °C are 0.25−1.85×10^{-2} (s^{-1}). It is worth noting that the Co_3O_4/ZSM-5 catalyst prepared hydrothermally is more active than other noble metal (Pd, Pt, and Rh) catalysts for propane oxidation. For instance, the TOF of the HT catalyst at 230 °C is 1.85×10^{-2} (s^{-1}) and is much higher than that of Pd/ZSM-5 (3.6×10^{-3} s^{-1}) at 280 °C and Pt/MgO (8.3×10^{-3} s^{-1}) at 260 °C.[51] Therefore, the Co_3O_4/ZSM-5 catalyst is a very promising potential catalyst for propane oxidation.

For propane oxidation on cobalt oxide-based catalysts, a number of parameters of catalyst, such as the crystallite size, surface area, reducibility of the cobalt species, the nature of the support, and the cobalt content on the support, are thought to

Table 5. T_{50}, T_{90}, Reaction Rates (r) and Activation Energies (E_a) and TOFs of Catalysts for Propane Oxidation at 230 °C

			$r \times 10^7$		$r_{surf} \times 10^9$			
catalyst	T_{50} (°C)[a]	T_{90} (°C)[a]	mol/(g_{cat}·s)	mol/($g_{Co_3O_4}$·s)	mol/(m_{cat}^2 s)	mol/(m_{Co}^2 s)	TOF × 10^2 (s^{-1})	E_a (kJ/mol)
IM	277	314	0.65	1.99	0.38	0.61	0.25	104
DP-Na	256	287	1.69	5.09	0.68	2.41	1.00	96.5
DP-NH	238	274	3.45	10.7	1.12	3.52	1.45	81.3
HT	235	260	3.67	11.1	1.17	4.48	1.85	79.7
Co_3O_4	455		0.40	0.40	1.40			62.8
Pd/ZSM-5[b]	326	332	0.12	8.82[c]	0.043	0.02[d]	0.36	106

[a]Reaction temperature of 50% or 90% propane conversion. [b]Reaction temperature is 280 °C. [c]The unit is mol/(g_{Pd}s). [d]The unit is mol/(m_{Pd}^2s).

dx.doi.org/10.1021/cs400068v | ACS Catal. 2013, 3, 1154−1164

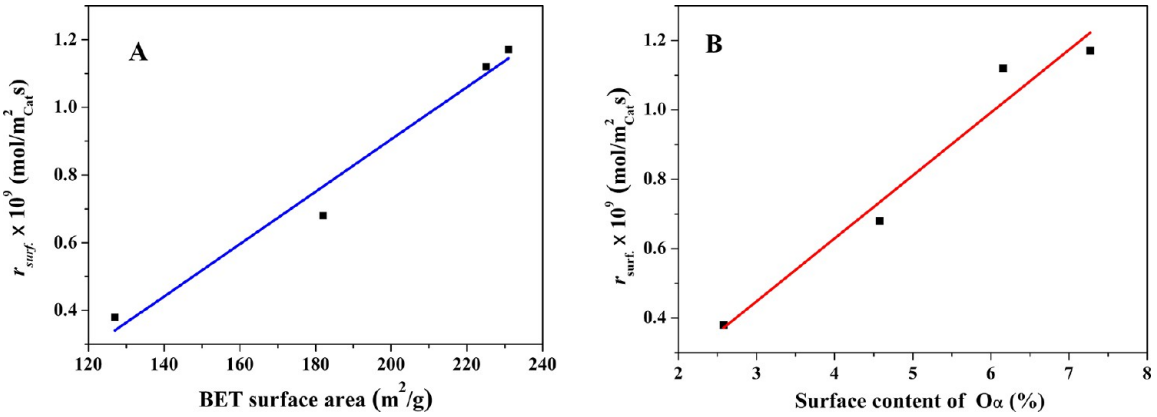

Figure 11. Influence of the surface area (*A*) and the surface O_α content (*B*) on the areal rate over Co_3O_4/ZSM-5 catalysts.

affect the catalytic performance.[11,49] Although the catalytic activity of the Co_3O_4/ZSM-5 catalyst is increased with an increase in the crystallite size of Co_3O_4 on the DP-Na (16.4 nm), DP-NH (16.9 nm), and HT (35.4 nm) catalysts, the IM catalyst with a larger crystallite size of Co_3O_4 (31.2 nm) exhibits a much lower activity than DP-NH and DP-Na catalysts. Thus, the catalytic activity could not be correlated to the crystallite size of the Co_3O_4 on ZSM-5. However, an analogous linear relationship between the reaction rates per surface area and BET surface areas of Co_3O_4/ZSM-5 catalysts can be found (Figure.11A), and the areal rates are increased with an increase in the surface area. The HT catalyst with the highest surface area exhibits a higher specific rate ($r_{surf} = 1.17 \times 10^{-9}$ mol/(m_{Cat}^2·s)) at 230 °C, which is above three times higher than that of the IM catalyst.

Generally, the catalytic activity is thought to be related to the reducibility of the active sites for the deep oxidation of short chain alkanes. Here, it has been observed that the reducibility of Co^{3+} on the Co_3O_4/ZSM-5 catalysts is varied in the order of HT > DP-NH > DP-Na > IM (Figure 5 and Table 2), but the order for Co^{2+} reducibility is HT > IM > DP-NH > DP-Na. The difference in the above order between the Co^{3+} and Co^{2+} reducibility can be well explained by the FT-IR spectra of Co_3O_4/ZSM-5 catalysts. As shown in Figure 6, the stretching vibration band of Co^{3+}−O at ∼575 cm^{-1} is changed in the order of HT(565 cm^{-1}) < DP-NH(569) < DP-Na(573) < IM(575), and the stretching vibration band of Co^{2+}−O at ∼667 cm^{-1} varies in the order of HT(665 cm^{-1}) = IM(665) < DP-NH(667) = DP-Na(667). It has been reported that the stretching vibration band shifted to a lower wavenumber means a decrease in the Co−O bond strength in Co_3O_4.[37,50] Thus, the catalyst with the lower wavenumber of vibration band of Co^{3+}−O (or Co^{2+}−O) shows the easier reduction of the Co^{3+}−O (or Co^{2+}−O) bond. On the basis of the fact mentioned above that the rate of propane oxidation over Co_3O_4/ZSM-5 catalysts is decreased in the order of $r_{HT} > r_{DP\text{-}NH} > r_{DP\text{-}Na} > r_{IM}$, it can be concluded that the Co^{3+} reducibility is responsible for the catalytic activity, and a high reducibility of Co^{3+} leads to a higher catalytic activity (or higher reaction rate) of Co_3O_4/ZSM-5. It is also found that the variation of the catalytic activity of Co_3O_4/ZSM-5 catalysts parallels the relative content of surface Co^{3+} (Figure 12); its order is HT > DP-NH > DP-Na > IM.

It was reported that hydrocarbon oxidation over metal oxides occurs through a Mars−Van Krevelen mechanism involving the participation of a lattice oxygen by a redox cycle.[50,52] Recently, Solsona et al. reported that lattice O^{2-} anions participated in the total oxidation of propane over the Co_3O_4 catalyst according to a

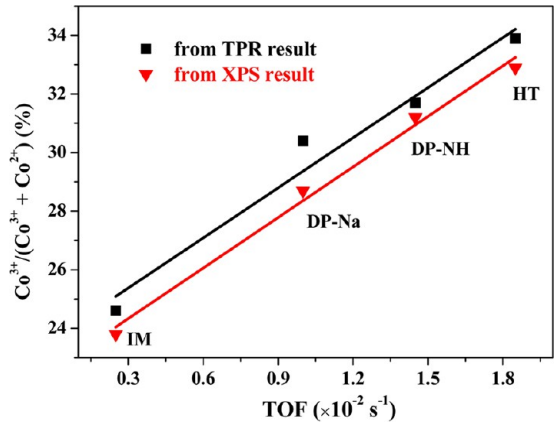

Figure 12. The relation between TOF and $Co^{3+}/(Co^{3+} + Co^{2+})$ calculated by TPR and XPS.

Mars−Van Krevelen mechanism.[50] For the combustion of methane over the cobalt oxide catalyst, it also follows a Mars−Van Krevelen mechanism and depends on the fast migration of oxygen ions through the lattice of cobalt oxide.[53] Herein, the correlation between the surface content of the lattice oxygen (O_α) of Co_3O_4 and the areal rate ($r_{surf.}$) of Co_3O_4/ZSM-5 catalysts can also be established in Figure 11B, and the catalyst (such as the HT catalyst) with more O_α content exhibits a higher areal rate; that is to say, the concentration of O_α is another significant factor to sustain the higher catalytic activity of the Co_3O_4/ZSM-5 catalyst. No linear correlation between the reaction rates and the surface adsorbed oxygen (O_β) amounts can be established because the DP-NH catalyst with the highest surface O_β content (11.0%) shows lower reaction rates than the HT catalyst with the surface O_β content of 8.5%. On the basis of the research results above, it can be considered that the propane oxidation over the Co_3O_4/ZSM-5 catalyst keeps to the Mars−Van Krevelen redox mechanism.

3.6. Stability of Catalyst for the Propane Oxidation. It has been reported that a thermal deactivation is one of the major reasons for the limited application of the cobalt oxide catalyst[21] because an exposure at high temperature will cause crystal growth and a loss of surface area, resulting in a fast drop in the catalytic activity. Herein, the catalytic performances of HT and IM catalysts were tested at different reaction temperatures for propane oxidation. The results in Figure 13 show that, using the HT catalyst, 58% propane conversion can be obtained after 3 h at 240 °C. To evaluate the thermal stability of the HT catalyst, the

dx.doi.org/10.1021/cs400068v | ACS Catal. 2013, 3, 1154−1164

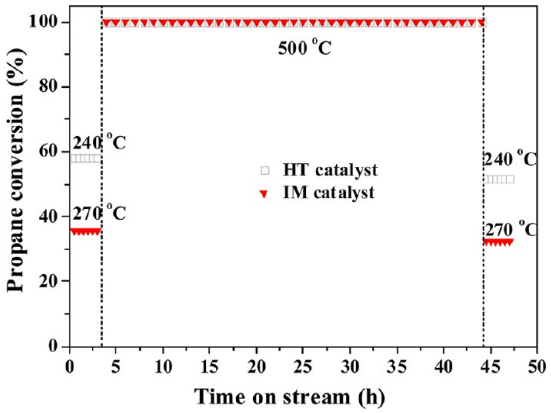

Figure 13. Propane conversion as a function of the reaction temperature over the HT and IM catalysts.

reaction temperature was increased to 500 °C and maintained at this temperature for 40 h. The propane conversion of ~100% was maintained, and no deactivation of the HT catalyst was found. Then the reaction temperature was reduced to 240 °C for 3 h, and a propane conversion of 51% was obtained, which is only slightly lower than the 58% propane conversion over the fresh catalyst.

The thermal stability of the IM catalyst was also tested in a way similar to that of the HT catalyst. The results in Figure 13 indicate that after the IM catalyst was operated at 500 °C for 40 h, the propane conversion at 270 °C was reduced from 35% to 32%. It was reported that the propane conversion over the Co_3O_4 catalyst was decreased from 80% to 60−65% after being used at 475 °C for 30 h as a result of sintering and agglomeration of the Co active phase or species.[50] Liu et al. reported also that an evident deactivation of Co_3O_4 catalyst was observed after it was used at 500 °C for 10 h, in which propane conversion dropped from 74% to 50% as a result of a decrease in the surface area of catalyst.[49] Our results above show that the Co_3O_4/ZSM-5 catalysts exhibit excellent catalytic activity and thermal stability for propane oxidation. The XRD patterns and surface areas of the HT and IM catalysts used at 500 °C for 40 h were tested and are shown in Figure 14 and Table 6. The results show that the XRD patterns of HT and IM catalysts used at 500 °C for 40 h are almost the same as that of fresh HT and IM catalysts, and their surface areas and crystallite sizes are decreased little compared

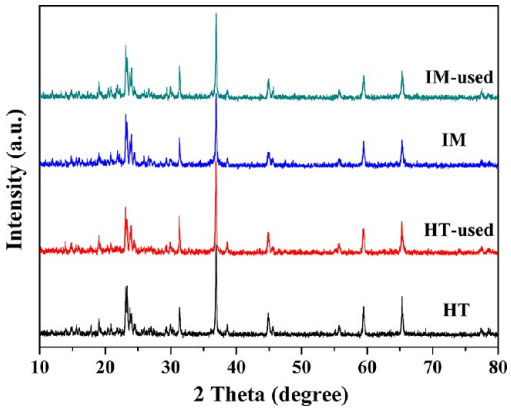

Figure 14. XRD patterns of HT and IM catalysts before and after being used.

Table 6. BET Surface Areas and Crystallite Sizes of IM and HT Catalysts before and after Testing

	surface area (m^2/g)		particle size (nm)	
sample	fresh	used at 500 °C for 40 h	fresh	used at 500 °C for 40 h
IM	127	125	31.2	33.2
HT	231	222	35.4	39.8

with that of fresh catalysts, which can well explain the slight decrease in the catalytic activity of the catalyst used.

4. CONCLUSIONS

In summary, the Co_3O_4/ZSM-5 catalysts prepared by different methods exhibit much higher catalytic activity than the Pd/ZSM-5 catalyst for propane oxidation. For instance, T_{50} and T_{90} over the Pd/ZSM-5 catalyst are 326 and 332 °C, and T_{50} and T_{90} over the HT catalyst are only 235 and 260 °C, respectively. The preparation method also seriously influences the catalytic activity of the Co_3O_4/ZSM-5 catalyst. The Co_3O_4/ZSM-5 catalyst prepared hydrothermally exhibits the highest catalytic activity and the highest areal rates among the four Co_3O_4/ZSM-5 catalysts. The Co_3O_4/ZSM-5 catalyst (DP) prepared by the deposition precipitation method displays catalytic activity that is superior to that of the catalyst created by an impregnation method, and the precipitant has an evident influence on its catalytic activity. For instance, the DP-NH catalyst prepared with ammonium bicarbonate precipitant exhibits a higher areal rate than the DP-Na catalyst prepared with the sodium hydroxide precipitant.

The excellent catalytic activity of Co_3O_4/ZSM-5 catalysts can be attributed to the easy reducibility of Co^{3+}, higher Co^{3+} content, higher surface content of lattice oxygen, and fast migration of oxygen ions in the lattice of cobalt oxide. The different preparation methods can obviously affect the physicochemical properties of Co_3O_4/ZSM-5 catalyst, resulting in its catalytic performance. The propane oxidation over Co_3O_4/ZSM-5 catalysts follows the Mars−Van Krevelen redox mechanism. Co_3O_4/ZSM-5 catalysts also possess remarkable thermal stability under the conditions used in propane oxidation. The catalytic activity of Co_3O_4/ZSM-5 catalysts is decreased a little after online test at 500 °C for 40 h, which can be attributed to the slight variation of the surface area and crystalline size of the Co_3O_4/ZSM-5 catalyst. Therefore, the Co_3O_4/ZSM-5 catalyst is a very promising potential catalyst for propane oxidation.

AUTHOR INFORMATION

Corresponding Author

*Fax: +86-21-64253824. E-mail: gzhlu@ecust.edu.cn.

Notes

The authors declare no competing financial interest.

ACKNOWLEDGMENTS

We would like to acknowledge financial support from the National Basic Research Program of China (2010CB732300, 2013CB933201), the National Natural Science Foundation of China (21273150), the Fundamental Research Funds for the Central Universities, the National High Technology Research and Development Program of China (2012AA062703), and the "Shu Guang" Project (10GG23) of the Shanghai Municipal Education Commission and Shanghai Education Development Foundation.

REFERENCES

(1) Garcia, T.; Solsona, B.; Murphy, D. M.; Antcliff, K. L.; Taylor, S. H. *J. Catal.* **2005**, *229*, 1−11.
(2) Taylor, M. N.; Zhou, W.; Garcia, T.; Solsona, B.; Carley, A. F.; Kiely, C. J.; Taylor, S. H. *J. Catal.* **2012**, *285*, 103−114.
(3) Solsona, B.; Aylon, E.; Murillo, R.; Mastral, A. M.; Monzonis, A.; Agouram, S.; Davies, T. E.; Taylor, S. H.; Garcia, T. *J. Hazard. Mater.* **2011**, *187*, 544−552.
(4) Kim, D. J.; Kim, J. M.; Yie, J. E.; Seo, S. G.; Kim, S. C. *J. Colloid Interface Sci.* **2004**, *274*, 538−542.
(5) Okal, J.; Zawadzki, M.; Tylus, W. *Appl. Catal., B* **2011**, *101*, 548−559.
(6) Okal, J.; Zawadzki, M. *Appl. Catal., B* **2011**, *105*, 182−190.
(7) Sanz, O.; Delgado, J. J.; Navarro, P.; Arzamendi, G.; Gandia, L. M.; Montes, M. *Appl. Catal., B* **2011**, *110*, 231−237.
(8) Ran, R.; Weng, D.; Wu, X. D.; Fan, J.; Qing, L. *Catal. Today* **2007**, *126*, 394−399.
(9) Rida, K.; Benabbas, A.; Bouremmad, F.; Pen, M. A.; Sastre, E.; Arias, A. M. *Appl. Catal., B* **2008**, *84*, 457−467.
(10) Zavyalova, U.; Nigrovski, B.; Pollok, K.; Langenhorst, F.; Muller, B.; Scholz, P.; Ondruschka, B. *Appl. Catal., B* **2008**, *83*, 221−228.
(11) Cheng, J.; Yu, J. J.; Wang, X. P.; Li, L. D.; Li, J. J.; Hao, Z. P. *Energy Fuels* **2008**, *22*, 2131−2137.
(12) Milt, V. G.; Ulla, M. A.; Lombardo, E. A. *Catal. Lett.* **2000**, *65*, 67−73.
(13) Baldi, M.; Finocchio, E.; Milella, F.; Busca, G. *Appl. Catal., B* **1998**, *16*, 43−51.
(14) Busca, G.; Daturi, M.; Finocchio, E.; Lorenzelli, V.; Ramis, G.; Willey, R. J. *Catal. Today* **1997**, *33*, 239−249.
(15) Solsona, B.; Vazquez, I.; Garcia, T.; Davies, T. E.; Taylor, S. H. *Catal. Lett.* **2007**, *116*, 116−121.
(16) Zavyalova, U.; Scholz, P.; Ondruschka, B. *Appl. Catal., A* **2007**, *323*, 226−233.
(17) Vob, M.; Borgmann, D.; Wedler, G. *J. Catal.* **2002**, *212*, 10−21.
(18) Tsoncheva, T.; Lvanova, L.; Rosenholm, J.; Linden, M. *Appl. Catal., B* **2009**, *89*, 365−374.
(19) Khodakov, A. Y.; Chu, W.; Fongarland, P. *Chem. Rev.* **2007**, *107*, 1692−1744.
(20) Luo, J. Y.; Meng, M.; Yao, J. S.; Li, X. G.; Zha, Y. Q.; Wang, X. T.; Zhang, T. Y. *Appl. Catal., B* **2009**, *87*, 92−103.
(21) Liotta, L. F.; Carlo, G. D.; Pantaleo, G.; Deganello, G. *Appl. Catal., B* **2007**, *70*, 314−322.
(22) Kanazawa, T. *Appl. Catal., B* **2006**, *65*, 185−190.
(23) Bessell, S. *Appl. Catal., A* **1995**, *126*, 235−244.
(24) Abu-Zied, B. M.; Schwieger, W. *Appl. Catal., B* **2009**, *85*, 120−130.
(25) Abu-Zied, B. M.; Schwieger, W.; Unger, A. *Appl. Catal., B* **2008**, *84*, 277−288.
(26) Pieterse, J. A. Z.; Van den Brink, R. W.; Booneveld, S.; De Bruijn, F. A. *Appl. Catal., B* **2002**, *39*, 167−179.
(27) Liu, X. S.; Lampert, J. K.; Arendarskiia, D. A.; Farrauto, R. J. *Appl. Catal., B* **2001**, *35*, 125−136.
(28) Geng, Y.; Zhang, J. X.; Zhang, M. X.; Liu, L. C.; Zi, X. H.; He, H. *China Ind. Catal.* **2010**, *18*, 64−69.
(29) Spadaro, L.; Arena, F.; Granados, M. L.; Ojeda, M.; Fierro, J. L. G.; Frusteri, F. *J. Catal.* **2005**, *234*, 451−462.
(30) Paredes, J. R.; Diaz, E.; Diez, F. V.; Ordonez, S. *Energy Fuels* **2009**, *23*, 86−94.
(31) Alvarez, J.; Ordonez, S.; Rosal, R.; Sastre, H.; Diez, F. V. *Appl. Catal., A* **1999**, *180*, 399−409.
(32) Ordonez, S.; Sastre, H.; Diez, F. V. *Appl. Catal., B* **2001**, *29*, 263−273.
(33) Arnoldy, P.; Moulijn, J. A. *J. Catal.* **1985**, *93*, 38−54.
(34) Liotta, L. F.; Carlo, G. D.; Pantaleo, G.; Venezia, A. M.; Deganello, G. *Appl. Catal., B* **2006**, *66*, 217−227.
(35) Xue, L.; Zhang, C. B.; He, H.; Teraoka, Y. *Appl. Catal., B* **2007**, *75*, 167−174.
(36) De Rivas, B.; Lopez-Fonseca, R.; Gonzalez-Jimeniz, C.; Gutierrez-Ortiz, J. I. *J. Catal.* **2011**, *281*, 88−97.
(37) Tang, C. W.; Kuo, C. C.; Kuo, M. C.; Wang, C. B.; Chien, S. H. *Appl. Catal., A* **2006**, *309*, 37−43.
(38) Yan, Q. Y.; Li, X. Y.; Zhao, Q. D.; Chen, G. H. *J. Hazard. Mater.* **2012**, *209−210*, 385−391.
(39) Jacobs, G.; Ji, Y. Y.; Davis, B. H.; Cronauer, D.; Kropf, A. J.; Marshall, C. L. *Appl. Catal., A* **2007**, *333*, 177−191.
(40) Khodakov, A. Y.; Constant, A. G.; Bechara, R.; Villain, F. *J. Phys. Chem. B.* **2001**, *105*, 9805−9811.
(41) Baylet, A.; Royer, S.; Marecot, P.; Tatibouet, J. M.; Duprez, D. *Appl. Catal., B* **2008**, *81*, 88−96.
(42) He, T.; Chen, D. R.; Jiao, X. L.; Wang, Y. L.; Duan, Y. Z. *Chem. Mater.* **2005**, *17*, 4023−4030.
(43) Niasari, M. S.; Mir, N.; Davar, F. *J. Phys. Chem. Solids* **2009**, *70*, 847−852.
(44) Hou, X. D.; Wang, Y. Z.; Zhao, Y. X. *Catal. Lett.* **2008**, *123*, 321−326.
(45) Ozvatan, S.; Yurum, Y. *Energ. Source* **2001**, *23*, 475−485.
(46) Luo, J. Y.; Meng, M.; Li, X.; Li, X. G.; Zha, Y. Q.; Hu, T. D.; Xie, Y. N.; Zhang, J. *J. Catal.* **2008**, *254*, 310−324.
(47) Xue, N. H.; Nie, L.; Fang, D. M.; Guo, X. F.; Shen, J. Y.; Ding, W. P.; Chen, Y. *Appl. Catal., A* **2009**, *352*, 87−94.
(48) He, L. F.; Liu, J. D.; Huang, W.; Li, Z. *Chem. J. Chin. Univ.* **2012**, *33*, 2532−2536.
(49) Liu, Q.; Wang, L. C.; Cao, Y.; Chen, M.; He, H. Y.; Fan, K. N. *J. Catal.* **2009**, *263*, 104−113.
(50) Solsona, B.; Davies, T. E.; Garcia, T.; Vazquez, I.; Dejoz, A.; Taylor, S. H. *Appl. Catal., B* **2008**, *84*, 176−184.
(51) Garetto, T. F.; Rincon, E.; Apesteguia, C. R. *Appl. Catal., B* **2004**, *48*, 167−174.
(52) Song, K. S.; Klvana, D.; Kirchnerova, J. *Appl. Catal., A* **2001**, *213*, 113−121.
(53) Bahlawaue, N. *Appl. Catal., B* **2006**, *67*, 168−176.